*Proc. Natl. Acad. Sci. USA*
Vol. 90, pp. 9896–9900, November 1993
Neurobiology

# Localized $^1$H NMR measurement of glucose consumption in the human brain during visual stimulation

(cerebral metabolic rate of glucose/brain activity/cerebral metabolism/visual cortex)

WEI CHEN*, EDWARD J. NOVOTNY†, XIAO-HONG ZHU*, DOUGLAS L. ROTHMAN‡, AND R. G. SHULMAN*

Departments of *Molecular Biophysics and Biochemistry, ‡Internal Medicine, and †Pediatrics, Yale University School of Medicine, New Haven, CT 06510

*Contributed by R. G. Shulman, July 15, 1993*

ABSTRACT **Spatially localized $^1$H NMR spectroscopy has been applied to measure changes in brain glucose concentration during 8-Hz photic stimulation. NMR spectroscopic measurements were made in a 12-cm$^3$ volume centered on the calcarine fissure and encompassing the primary visual cortex. The average maximum change in glucose levels was 0.34 $\mu$mol·g$^{-1}$ ($n$ = 5) at 15 min; glucose level had turned toward resting level at 25 min. The glucose change was used to calculate the increase of glucose cerebral metabolic rate in the visual cortex region for individual subjects by using the Michaelis–Menten model of glucose transport on the assumption of constant transport kinetics. The glucose cerebral metabolic rate was calculated to increase over the nonstimulated rate by 22% during the first 15 min of photic stimulation. A model in which the glucose metabolic rate gradually decreases during stimulation was proposed as a possible explanation for the recovery of brain glucose and previously measured lactate concentrations to prestimulus values after 15 min.**

Glucose is the major carbon source for brain energy metabolism (1). A variety of methods have been developed for studying glucose metabolism *in vivo* in humans, including radiolabeling methods such as positron emission tomography (PET) (2), which is based on the deoxyglucose autoradiography method of Sokoloff *et al.* (3, 4), and more recently *in vivo* NMR (5–7). Recent studies have examined glucose metabolism during functional activation. Fox *et al.* (8) reported a mean increase of 51% in the cerebral metabolic rate of glucose ($CMR_{Glc}$) of visual cortex during stimulation by a flashing checkerboard pattern using PET. This value was accompanied by a negligible increase in the cerebral metabolic rate of oxygen ($CMR_{O_2}$), leading the authors to suggest that the increase in $CMR_{Glc}$ was entirely due to anaerobic glycolysis. Such a result appears to contradict the traditional view of brain metabolism, in which glucose oxidation is considered to be the primary energy-producing pathway in resting brain.

To test this PET finding we had previously obtained $^1$H NMR spectra of the visual cortex during visual stimulation (5). A substantial amount of lactate would be expected to accumulate if anaerobic glycolysis persisted at the reported rate for the full 40 min required for the PET measurement. In accordance with the PET results, the NMR study showed an increase in lactate concentration (5). However, the observed increase ($\leq$0.4 mM) was smaller than predicted from the reported increase in $CMR_{Glc}$ and reached a maximum within the first spectrum after the start of stimulation (6 min); thereafter lactate concentration declined for $\approx$15–20 min (5); similar findings have been reported by other groups (9, 10).

Although the qualitative observation of lactate elevation agreed with the PET measurements, the increase in lactate concentration was less than that predicted were anaerobic glycolysis to persist for 40 min. To understand the time course of lactate and metabolism during visual stimulation we reasoned that measurement of the time dependence of $CMR_{Glc}$ in the visual cortex was necessary. Because the PET measurement of $CMR_{Glc}$ was an average over 40 min (8), a recovery of $CMR_{Glc}$ with time would not be detected, and this may explain the leveling and decline of brain lactate levels. Regional $^1$H NMR measurements of intracerebral glucose concentration provided a potential method for continuously measuring $CMR_{Glc}$.

From previous studies, particularly of the rat brain (11, 12), a model had been proposed and evaluated that relates cerebral glucose concentration to the kinetics of glucose transport across the blood–brain barrier, the plasma glucose concentration, and $CMR_{Glc}$. This model assumed reversible, saturable glucose transporters that behaved according to Michaelis–Menten kinetics (11). We have recently determined the kinetic parameters of this model for human brain by two different *in vivo* NMR experiments. (*i*) In the first experiment [1-$^{13}$C]glucose was infused, and brain glucose concentration was measured by $^{13}$C NMR under steady-state conditions (6). From measurements of brain glucose concentration as a function of plasma glucose levels, analysis of the data determined the glucose-transport kinetic parameters $K_T$ and $T_{max}$ (see *$CMR_{Glc}$ Calculation*). (*ii*) The second experiment was a transient kinetic experiment in which plasma glucose concentration ($G_o$) was raised rapidly, and the time course of glucose appearance in the brain was measured by $^1$H NMR difference spectroscopy (13). Determination of the kinetic parameters with this technique gave values of $K_T$ and $T_{max}$ consistent with those derived from the steady-state measurements, which supports the model of transport and the derived kinetic parameters. In this paper we measure brain glucose concentration by $^1$H NMR and use these values to calculate the time dependence of $CMR_{Glc}$ during visual stimulation.

## MATERIALS AND METHODS

**Spectroscopy.** The localized $^1$H NMR spectra were obtained with a modified Bruker Biospec I spectrometer (Bruker, Billerica, MA) equipped with a 2.1-T 1-m bore magnet and shielded gradients (Oxford Magnet Technology, Oxford, U.K.). The surface-coil probe consisted of a $^1$H coil (diameter, 6 cm) for transmission and reception. Volume selection of a localized $^1$H spectrum within brain visual cortex was guided by sagittal and transverse $T_1$ weighted-gradient echo image. An automated shimming routine (for optimizing field homogeneity) was used as described in ref. 14. The localized volume was 12 cm$^3$ (3 × 2 × 2 cm$^3$), as shown in Fig. 1. The localized volume covered most of the

The publication costs of this article were defrayed in part by page charge payment. This article must therefore be hereby marked "*advertisement*" in accordance with 18 U.S.C. §1734 solely to indicate this fact.

Abbreviations: PET, positron emission tomography; $CMR_{O_2}$, cerebral metabolic rate of oxygen; $CMR_{Glc}$, cerebral metabolic rate of glucose; $CMR_{Glc,ps}$, cerebral metabolic rate of glucose during photic stimulation.

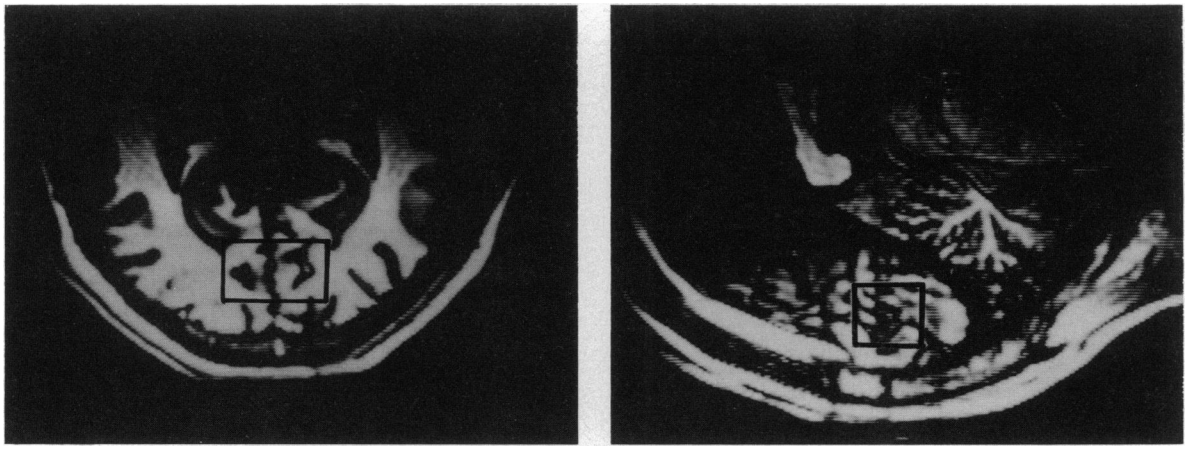

FIG. 1. The $T_1$ weighted transverse (*Left*) and sagittal (*Right*) imagings at repetition time (TR) = 2.5 sec, inversion time (TI) = 0.75 sec, and echo time (TE) = 14 ms. The boxes show the localized volume of 3 cm × 2 cm × 2 cm (12 $cm^3$).

primary visual cortex region by centering on the calcarine fissure. The pulse sequence was similar to that used previously for $^1H$ NMR brain glucose measurements (15). Volume selection was achieved by the three-dimensional image-selected *in vivo* spectroscopy technique (16) using 8-msec hyperbolic secant pulses (the pulse parameter $\mu = 5$, bandwidth 2 kHz) (17). Outer volume contamination was suppressed by noise pulses (18) in the two planes perpendicular to the surface coil. The lipid was suppressed by using a curved surface-spoiler gradient (19) and a $\theta/3$ pulse before the localization sequence (20). A sinc pulse was applied for slice-selected excitation on the plane parallel to the coil. Water suppression was achieved by using a 2-2 semiselective refocusing pulse (21), which optimizes signals around the glucose region at 3.44 ppm and a low-power presaturation during the recovery period. The echo time (TE) was 16 msec and repetition time (TR) was 2.8 sec. The spectra were collected in 3.3-min time resolution (64 scans). Usually 6 control spectra and 9–10 spectra during visual stimulation were acquired. In some cases, 5 spectra were acquired after stimulation.

***In vivo* NMR Data Processing.** All free induction decays were processed by 32,000 zero filling and Fourier transformation. To correct the glucose intensity due to the effect of the frequency-selective excitation profile of the semiselective refocusing pulse and the signal loss due to spin–spin coupling modulation, the pulse sequence was applied to a phantom containing equimolar glucose and creatine at 37°C. The integrated intensity ratio of glucose at 3.44 ppm to creatine at 3.03 ppm was determined under fully relaxed conditions and used to calculate the glucose-to-creatine concentration ratio *in vivo*. Comparison of the $T_1$ relaxation time differences of glucose and creatine between *in vivo* and *in vitro* indicates that the integrated ratio obtained from the phantom at full relaxation should provide an accurate correction for *in vivo* glucose quantification. The peak at 3.03 ppm in human brain was assumed to be of constant intensity, arising from 10 mM creatine (22). The change of glucose concentration during stimulation was obtained by comparing the difference of peak integration between the control and stimulated spectra at 3.40–3.48 ppm and converting to concentration by comparison with the corrected creatine intensity.

**$CMR_{Glc}$ Calculation.** The Michaelis–Menten glucose-transport model (Lund–Anderson) as shown in Fig. 2 was used for calculating $CMR_{Glc}$. The flow equation, balancing input and output from the brain glucose ($G_i$) pool is

$$dG_i/dt = T_{in} - T_{out} - CMR_{Glc} \quad [1]$$

and

$$T_{in} = G_o T_{max}/(G_o + K_T)$$

$$T_{out} = G_i T_{max}/(G_i + K_T),$$

where $G_o$ is plasma glucose concentration, $T_{in}$ and $T_{out}$ are transport rates into and out of the brain, respectively, and $K_T$ is the Michaelis–Menter half-saturation constant. Eq. 1 has been used to calculate the $T_{max}/CMR_{Glc}$ ratio and the $K_T$ constant for human brain at steady-state glucose concentration (6). This equation shows that a steady-state increase in $CMR_{Glc}$ will require a steady-state decrease in $G_i$. This relationship suggests that Eq. 1 could be used to calculate $CMR_{Glc}$ by using the measured values of $G_i$ as an input function. The calculation depends on the assumption that the transport parameters reported previously remain constant during visual stimulation. The measured change in $G_i$ upon visual stimulation provides a determination of the change in $CMR_{Glc}$.

To determine $CMR_{Glc}$, the *in vivo* brain glucose concentration ($G_i$) was measured versus time of stimulation. Values assumed from previous measurements to calculate $CMR_{Glc}$ were as follows: the Michaelis–Menten half-saturation constant $K_T = 4.9$ mM, the $T_{max}/CMR_{Glc}$ ratio = 3.6, $G_o = 5$ mM, the initial $G_i = 1.1$ $\mu mol \cdot g^{-1}$ (6), and $CMR_{Glc} = 0.42$ $\mu mol \cdot g^{-1} \cdot min^{-1}$ (8), where g refers to gram of brain tissue. For calculations, the values of $G_i$ and $CMR_{Glc}$ were converted to units of $\mu mol \cdot ml^{-1}$, where ml refers to ml of water volume in brain tissue, using a correction factor of 0.77 (6). The initial glucose concentration ($G_i$) determined from the transport kinetic constants and the plasma glucose concentration are not significantly different from the euglycemia $G_i$ values measured in the $^{13}C$ NMR study (6). To calculate the change

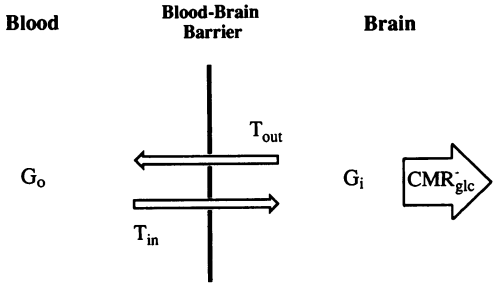


FIG. 2. Schematic demonstration of brain glucose-transport using Michaelis–Menten model. $G_o$, plasma glucose; $G_i$, brain glucose pool; $T_{in}$, inward transport rate; $T_{out}$, outward transport rate.

in $CMR_{Glc}$ a Runge–Kutta method was used to solve the glucose-transportation differential equation and a Nelder–Meade simplex algorithm (23) was used to optimize the fit of Eq. 1 to the experimental data by varying the $CMR_{Glc}$ value.

**Human Experiments.** Five separate studies were done on three volunteers; subjects gave written consent according to the protocol approved by the Yale Human Investigation Committee. Blood samples were obtained before and during the photic stimulation in two experiments to determine plasma glucose concentration $G_o$. The results of blood glucose level analysis with a Beckman glucose analyzer showed that $G_o$ did not change significantly before and during visual stimulation. Photic stimulation was presented through a goggle from grids of red-light-emitting diodes to each eye at intervals of 128 ms (8 Hz), a stimulus pattern that has been reported to give maximal stimulation (24, 25).

## RESULTS

Fig. 3 shows the control $^1H$ spectrum from human visual cortex region (bottom spectrum) and 3.3-min difference spectra between the control spectrum and subsequent spectra acquired during and after photic stimulation under conditions similar to those used by Fox *et al.* (8). This figure shows the resolved difference peak at 3.44 ppm (along the dashed line), a peak previously assigned to glucose (15, 26). The increases in the difference peaks are proportional to the decreases in glucose concentration. Fig. 3 shows that brain glucose decreases at the beginning of stimulation and returns to normal glucose level ≈10 min after prolonged stimulation stops. The positions of the calcarine fissure and primary visual cortex relative to the surface coil varied with different subjects and were determined from $T_1$ weighted images. To provide adequate sensitivity of quantification for each individual, three series of free induction decays were summed (10-min time resolution) for integration and $CMR_{Glc}$ simulations.

Glucose concentration changes during ≈30 min of visual stimulation for an individual subject are shown in Fig. 4. Changes in glucose concentration were determined from the change in intensity of the 3.44-ppm peak, which was normalized to the creatine integral that was assumed to represent 10 mM creatine concentration. The initial glucose concentrations was thus assumed to represent 1.1 $\mu mol \cdot g^{-1}$. Fig. 4 *Upper* shows the fitted glucose-transport curve and the $CMR_{Glc}$ value from one experiment using Eq. 1. Fig. 4 *Lower*

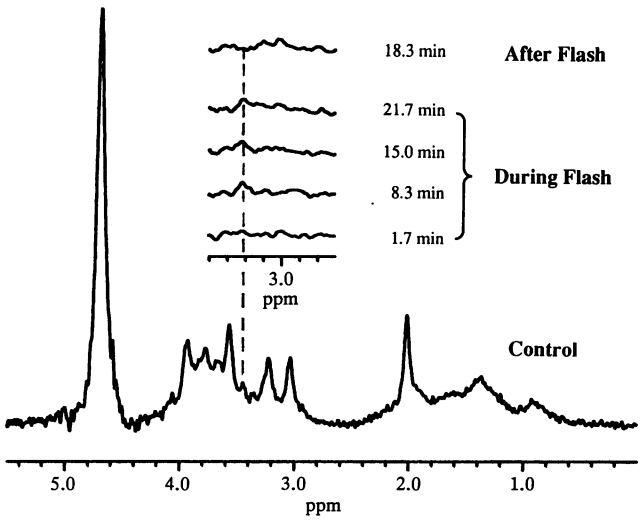


FIG. 3. Localized $^1H$ spectra (3.3-min time resolution) of visual cortex from human brain at resting situation (bottom trace, 0-Hz line broadening) and five difference peaks of glucose at 3.44 ppm during stimulation and after stimulation (5-Hz line broadening).

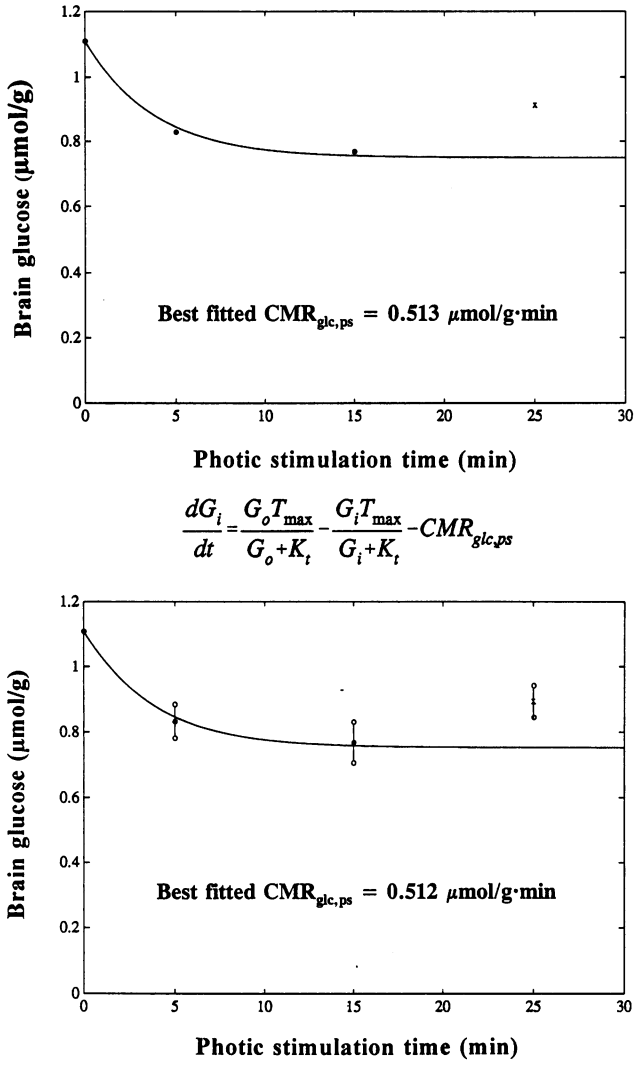


FIG. 4. (*Upper*) Curve simulation of glucose consumption rate during photic stimulation ($CMR_{Glc,ps}$) for one individual experiment. (*Lower*) Curve simulation of $CMR_{Glc,ps}$ for the average data set ($n$ = 5). A constant $CMR_{Glc,ps}$ model and the first three data points were used for the simulation.

is the curve fitted to the average of the five data sets. Although the first two measurements during visual stimulation show a progressive decrease in $G_i$, the third point taken ≈25 min after the start of stimulation clearly shows a return toward resting condition.

The return of $G_i$ toward resting values at the 25-min point does not agree with the glucose change expected from the Michaelis–Menten transport model of Eq. 1 for a constant value of $CMR_{Glc}$. For an approximation to the model, only the first three data points, including the initial $G_i$ were used to calculate the glucose consumption rate during photic stimulation ($CMR_{Glc,ps}$) by curve fitting to Eq. 1. The data from three subjects for $CMR_{Glc,ps}$ (in $\mu mol \cdot g^{-1} \cdot min^{-1}$) were as follows: subject 1, 0.48; subject 2, 0.55 and 0.55 in two trials; subject 3, 0.51 and 0.48 in two trials. These experiments assumed $CMR_{Glc}$ to equal 0.42 $\mu mol \cdot g^{-1} \cdot min^{-1}$. The average $CMR_{Glc,ps}$ value for the data from these three subjects is 0.51 ± 0.03 $\mu mol \cdot g^{-1} \cdot min^{-1}$.

It is observed that a single value of $CMR_{Glc,ps}$ fits the first three points of Fig. 4 during stimulation, which is consistent with a constant or slowly changing $CMR_{Glc,ps}$ during this period (0–15 min). The average $CMR_{Glc,ps}$ during the photic stimulation (8 Hz) was 0.51 ± 0.03 $\mu mol \cdot g^{-1} \cdot min^{-1}$ SD.

## DISCUSSION AND CONCLUSIONS

Localized $^1$H NMR spectroscopy with 12-cm$^3$ volume of interest has been applied to monitor the kinetics of cerebral glucose concentration during visual stimulation. During the first 15 min of stimulation the brain glucose concentration decreased, consistent with a constant increased value of $CMR_{Glc}$ during stimulation. After 25 min of stimulation the glucose concentration returned toward prestimulation levels.

Previously Merboldt *et al.* (26) had compared $^1$H NMR spectra of the human visual cortex with and without visual stimulation. They did not observe an increase in lactate concentration but reported a decrease in glucose concentration during stimulation. A difference spectrum they obtained from the summed data from seven subjects showed a decrease in the intensity at 3.44 ppm, which was estimated at ≈50% of resting glucose. Absence of a lactate elevation raised questions about these glucose changes, but our present results qualitatively agree with their glucose observations. More significantly the ability to obtain difference spectra on individual subjects (Fig. 3) due to the improved sensitivity of the present measurement has allowed analysis of the time dependence of intracerebral glucose. In conjunction with previous $^{13}$C and $^1$H NMR measurements of brain glucose-transport kinetics, this analysis allows calculation of the time course of $CMR_{Glc,ps}$ during photic stimulation.

The average maximal decrease of glucose concentration during photic stimulation was 0.34 $\mu$mol·g$^{-1}$ (a 31% decrease from the initial $G_i$ value of 1.1 $\mu$mol·g$^{-1}$) 15 min after stimulation started. This value is similar to the value of 0.4 $\mu$mol·g$^{-1}$ reported in the $^1$H NMR measurements of Merboldt *et al.* (26). They reported this decrease to represent 50% relative to a resting glucose concentration of 0.8 mM measured in the $^1$H NMR spectrum. However, using the $^{13}$C NMR-determined glucose concentration of 1.1 $\mu$mol·g$^{-1}$, the decrease in glucose they reported would correspond to a percentage change of ≈36%, which resembles our results. A regional decrease in glucose concentration with functional activation was reported by Ueki *et al.* (27) in rat brain during electrical stimulation of the paw.

Using the model described in the text, a value of $CMR_{Glc,ps}$ calculated during photic stimulation was 0.51 ± 0.03 $\mu$mol·g$^{-1}$·min$^{-1}$ ($n$ = 5) based on $CMR_{Glc}$ = 0.42 $\mu$mol·g$^{-1}$·min$^{-1}$ in resting visual cortex, a 22% increase. To assess sensitivity of the calculated percentage increase in $CMR_{Glc}$ to the assumed resting value, the computation was done with a range of reported values of $CMR_{Glc}$ (8, 28, 29). For $CMR_{Glc}$ between 0.30 and 0.42 $\mu$mol·g$^{-1}$·min$^{-1}$, the calculated value of $CMR_{Glc,ps}$ varied from 0.37 to 0.51 $\mu$mol·g$^{-1}$·min$^{-1}$, but percentage increase in $CMR_{Glc,ps}$ only ranged from 24 to 22%.

The calculated percentage increase in $CMR_{Glc,ps}$ is lower than the 51% increase during photic stimulation obtained from PET data (8). However, the most active region during stimulation of the visual cortex is in gray matter, as shown by high-resolution functional imaging studies (30). The localized NMR volume (12 cm$^3$) in the present experiments contains both gray and white matter, so that to the extent that glucose in white matter contributes to the NMR signal the fractional decrease in $G_i$ in the active region will be underestimated. In future studies it should be possible to quantitatively calculate the $CMR_{Glc}$ change by assessing the activated region within the spectroscopic volume with functional MRI (31, 32). However, although the magnitude of the change of $CMR_{Glc}$ may be underestimated by the present calculation, the time course of the change should be accurately represented.

All simulations were based on the assumption that the glucose-transport parameters did not change before and during visual stimulation. Were the glucose-transport parameters to change during visual stimulation, based on previous reports of animals under anesthesia (33) and during seizure (34), the apparent glucose-transport rate would be predicted to increase (e.g., increased $T_{max}$ or decreased $K_T$), resulting in a smaller decrease in brain glucose than predicted from constant transport parameters. Therefore, the effect of changes in transport kinetic parameters will cause an underestimate of $CMR_{Glc}$.

The time course of $G_i$ (Fig. 4) can be fit by assuming a constant elevated $CMR_{Glc}$ during the first 15 min of photic stimulation. However intracerebral glucose recovered to near prestimulation values during the latter stimulation period (≈25 min after starting stimulation). To assess whether the complete time course could be fit by a monotonically decreasing $CMR_{Glc,ps}$, the transport model was modified by assuming that $CMR_{Glc,ps}$ was described by the function $[1 + x\cdot\exp(-t/\tau)]$. Using four average data points for fitting the transport equations with time-dependent $CMR_{Glc,ps}$ gives $x$ = 0.27 and $\tau$ = 33 min based on $CMR_{Glc}$ = 0.42 $\mu$mol·g$^{-1}$·min$^{-1}$. The simulated curve fits the limited amount of experimental data well, as shown in Fig. 5.

The decay in $CMR_{Glc}$ is relatively slow, suggesting that a constant increased value of $CMR_{Glc,ps}$ during the initial stimulation period (0–15 min) is approximately valid. Because the reported lactate elevation reaches a maximum value in <3–6 min after the start of photic stimulation (5, 9, 10), a decline in $CMR_{Glc,ps}$ cannot explain the low maximum lactate level achieved. Alternate explanations are (*i*) an increase in lactate-transport rate, resulting in a new steady state or (*ii*) an increase in $CMR_{O_2}$ over this period to match the increase in glycolysis. Due to the much greater energy production from aerobic glycolysis these possibilities have dramatically different implications regarding the energy cost of functional activation.

The recovery of glucose levels by 25 min, which suggest a reduction in $CMR_{Glc,ps}$, parallels the previously observed decline in lactate elevation at this time. The reduced $CMR_{Glc,ps}$ could be due to a small increase in aerobic glycolysis or a decrease in functional energy requirements as the result of an adaptation process. Alternately there may be an alteration in transport parameters after long stimulation periods. These possibilities can be tested by using $^1$H-$^{13}$C NMR, as previously demonstrated (7, 28), to measure the rate of the tricarboxylic acid cycle during photic stimulation and direct $^1$H NMR (13) to measure transport parameters.

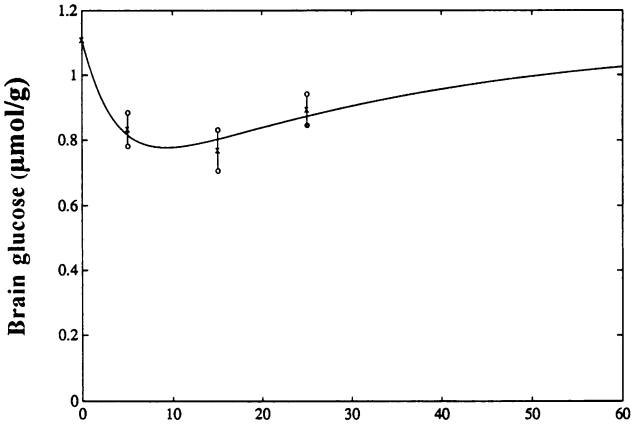


$$\frac{dG_i}{dt} = \frac{G_o T_{max}}{G_o + K_t} - \frac{G_i T_{max}}{G_i + K_t} - CMR_{glc}[1 + 0.27\exp(-t/\tau)]$$

FIG. 5. Curve simulation of $CMR_{Glc,ps}$ for the average data set ($n$ = 5). A variable $CMR_{Glc,ps}$ model and four data points were used for the simulation.

In conclusion, we have used localized $^1H$ NMR difference spectroscopy to measure the time course of brain glucose concentration during photic stimulation, and in combination with previously NMR-determined glucose-transport kinetics we have calculated the time dependence of $CMR_{Glc}$. The results show an approximately constant increased $CMR_{Glc}$ of a minimum of 22% during the first 15 min of photic stimulation. When partial volume effects are considered, the results are consistent with the previous PET report of a 51% increase of $CMR_{Glc}$ during photic stimulation and have an improved time resolution of 10 min. A model in which $CMR_{Glc}$ gradually decreases during stimulation was proposed as a possible explanation of the recovery of brain glucose and previously measured lactate concentrations to prestimulus values after 15 min.

Assistance from Dr. S. D. Boulware, Dr. M. J. Avison, and C. Ariyan is gratefully acknowledged. We express appreciation to Dr. Rolf Gruetter for assistance in pulse-sequence implementation. This work has been supported by Grant DK34576 from the National Institutes of Health, Bethesda, MD to R.G.S. and a grant from the Juvenile Diabetes Foundation to E.J.N.

1. Siesjo, B. K. (1978) in *Brain Energy Metabolism* (Wiley, New York), pp. 1–196.
2. Raichle, M. E. (1987) in *Handbook of Physiology: The Nervous System*, ed. Plum, F. (Am. Physiol. Soc., Bethesda, MD), Vol. 5, pp. 643–675.
3. Sokoloff, L., Reivich, M., Kennedy, C., Des Rosiers, M. H., Patlak, C. S., Pettigrew, K. D., Sakurada, O. & Shinohara, M. (1977) *J. Neurochem.* **28**, 897–916.
4. Sokoloff, L. (1981) *J. Cereb. Blood Flow Metab.* **1**, 7–36.
5. Prichard, J. W., Rothman, D., Novotny, E., Petroff, O., Kuwabara, T., Avison, M., Howseman, A., Hanstock, C. & Shulman, R. (1991) *Proc. Natl. Acad. Sci. USA* **88**, 5829–5831.
6. Gruetter, R., Novotny, S. D., Boulware, S. D., Rothman, D. L., Mason, G. F., Shulman, G. I., Shulman, R. G. & Tamborlane, W. V. (1992) *Proc. Natl. Acad. Sci. USA* **89**, 1109–1112.
7. Rothman, D. L., Novotny, E. J., Shulman, G. I., Howseman, A. M., Petroff, O. A. C., Mason, G. F., Nixon, T., Hanstock, C. C., Prichard, J. W. & Shulman, R. G. (1992) *Proc. Natl. Acad. Sci. USA* **89**, 9603–9606.
8. Fox, P. T., Raichle, M. E., Mintun, M. A. & Dence, C. (1988) *Science* **241**, 462–464.
9. Sappey-Marinier, D., Calabrese, G., Fein, G., Hugg, W., Biggins, C. & Weiner, M. W. (1992) *J. Cereb. Blood Flow Metab.* **12**, 584–592.
10. Jenkins, B. G., Belliveau, J. W. & Rosen, B. R. (1992) *Soc. Magn. Reson. Med. Abstr.* **11**, 2145.
11. Lund-Andersen, H. (1979) *Physiol. Rev.* **59**, 305–352.
12. Mason, G. F., Behar, K. L., Rothman, D. L. & Shulman, R. G. (1992) *J. Cereb. Blood Flow Metab.* **12**, 448–455.
13. Novotny, E. J., Gruetter, R., Rothman, D. L., Boulware, S. & Shulman, R. G. (1992) *Soc. Magn. Reson. Med. Abstr.* **11**, 1961.
14. Gruetter, R. & Boesch, C. (1992) *J. Magn. Reson.* **96**, 323–334.
15. Gruetter, R., Rothman, D. L., Novotny, S. D., Shulman, G. I., Prichard, J. W. & Shulman, R. G. (1992) *Magn. Reson. Med.* **27**, 183–188.
16. Ordidge, R. J., Conolley, A. & Lohman, J. A. B. (1986) *J. Magn. Reson.* **66**, 283–294.
17. Silver, M. S., Joseph, R. I., Chen, C. N., Sarky, V. J. & Hoult, D. I. (1984) *Nature (London)* **310**, 681–683.
18. Ordidge, R. J. (1987) *Magn. Reson. Med.* **5**, 93–98.
19. Chen, W. & Ackerman, J. J. H. (1989) *Nucl. Magn. Reson. Biomed.* **1**, 205–207.
20. Bendall, M. R. & Gordon, R. E. (1983) *J. Magn. Reson.* **53**, 365–385.
21. Hore, P. J. (1983) *J. Magn. Reson.* **55**, 283–300.
22. Petroff, O. A. C., Spencer, D. D., Alger, J. R. & Prichard, J. W. (1989) *Neurology* **39**, 1197–1202.
23. Dennis, J. E., Jr., & Woods, D. J. (1987) in *New Computing Environments: Microcomputers in Large-Scale Computing*, ed. by Wouk, A. (SIAM, Philadelphia), pp. 116–122.
24. Fox, P. T. & Raichle, M. E. (1984) *J. Neurophysiol.* **51**, 1109–1120.
25. Kwong, K. K., Belliveau, J. W., Chesler, D. A., Goldberg, I. E., Weisskoff, R. M., Ponceltet, B. P., Kennedy, D. N., Hoppel, B. E., Cohen, M. S., Turner, R., Cheng, H.-M., Brady, T. J. & Rosen, B. R. (1992) *Proc. Natl. Acad. Sci. USA* **89**, 5675–5679.
26. Merboldt, K.-D., Bruhn, H., Hanicke, W., Michaelis, T. & Frahm, J. (1992) *Magn. Reson. Med.* **25**, 187–194.
27. Ueki, M., Linn, F. & Hossmann, K.-A. (1988) *J. Cereb. Blood Flow Metab.* **8**, 486–494.
28. Schwartz, M., Duara, R., Haxby, J., Grady, C., White, B. J., Kessler, R. M., Kay, A. D., Culter, N. R. & Rapoport, S. I. (1983) *Science* **221**, 781–783.
29. Heiss, W.-D., Pawlik, G., Herholz, K., Wagner, R., Goldner, H. & Wienhard, K. (1984) *J. Cereb. Blood Flow Metab.* **4**, 212–223.
30. Ogawa, S., Tank, D. W., Menon, R., Ellermann, J., Kim, S.-G., Merkle, H. & Ugurbil, K. (1992) *Proc. Natl. Acad. Sci. USA* **89**, 5951–5955.
31. Belliveau, J. W., Kennedy, D. N., McKinstry, R. C., Buchbinder, B. R., Weisskoff, R. M., Cohen, M. S., Vevea, J. M., Brady, T. J. & Rosen, B. R. (1991) *Science* **254**, 716–719.
32. Blamire, A. M., Ogawa, S., Ugurbil, K., Rothman, D., McCarthy, G., Ellermann, J. M., Hyder, F., Rattner, Z. & Shulman, R. G. (1992) *Proc. Natl. Acad. Sci. USA* **89**, 11069–11073.
33. Gjedde, A. & Rasmussen, M. (1980) *J. Neurochem.* **35**, 1382–1387.
34. Borgstrom, L., Chapman, A. G. & Siesjo, B. K. (1976) *J. Neurochem.* **27**, 971–973.